Renewable Energy 132 (2019) 615–627

Contents lists available at ScienceDirect

Renewable Energy

journal homepage: www.elsevier.com/locate/renene

The role of glacier retreat for Swiss hydropower production

Bettina Schaefli [a, *], Pedro Manso [b], Mauro Fischer [c, d], Matthias Huss [c, e], Daniel Farinotti [e, f]

[a] Institute of Earth Surface Dynamics, University of Lausanne, Switzerland
[b] Laboratory of Hydraulic Constructions, School of Architecture, Civil and Environmental Engineering (ENAC), Ecole Polytechnique Fédérale de Lausanne (EPFL), Switzerland
[c] Department of Geosciences, University of Fribourg, Switzerland
[d] Department of Geography, University of Zürich, Switzerland
[e] Laboratory of Hydraulics, Hydrology and Glaciology, ETH Zurich, Switzerland
[f] Swiss Federal Institute for Forest, Snow and Landscape Research (WSL), Birmensdorf, Switzerland

ARTICLE INFO

Article history:
Received 1 February 2018
Received in revised form
12 July 2018
Accepted 21 July 2018
Available online 24 July 2018

Keywords:
Hydrology
Glacier mass balance
Hydropower
Climate change
Alps

ABSTRACT

High elevation or high latitude hydropower production (HP) strongly relies on water resources that are influenced by glacier melt and are thus highly sensitive to climate warming. Despite of the wide-spread glacier retreat since the development of HP infrastructure in the 20th century, little quantitative information is available about the role of glacier mass loss for HP. In this paper, we provide the first regional quantification for the share of Alpine hydropower production that directly relies on the waters released by glacier mass loss, i.e. on the depletion of long-term ice storage that cannot be replenished by precipitation in the coming decades. Based on the case of Switzerland (which produces over 50% of its electricity from hydropower), we show that since 1980, 3.0%–4.0% (1.0–1.4 TWh yr^{-1}) of the country-scale hydropower production was directly provided by the net glacier mass loss and that this share is likely to reduce substantially by 2040–2060. For the period 2070–2090, a production reduction of about 1.0 TWh yr^{-1} is anticipated. The highlighted strong regional differences, both in terms of HP share from glacier mass loss and in terms of timing of production decline, emphasize the need for similar analyses in other Alpine or high latitude regions.

© 2018 Elsevier Ltd. All rights reserved.

1. Introduction

Hydropower provides around 16% of the world's total electricity [1]. In the European Union, hydropower represented 11% of the gross electricity consumption of the 28 member states in 2016 [2] and high shares of hydropower production (HP) can in particular be found in high latitude and high elevation regions [3], where part of HP relies on water resources that are temporarily stored in the form of snow and ice, and are thus particularly vulnerable to climate warming [4].

Despite the well-known inherent variability of water resources availability, fundamental energy market models [5] but also large-scale hydropower assessments usually only account for selected baseline water years [6]. The notable exception are recent continental to global scale studies of HP potential [1] or of climate change impact on HP [7,8]. While giving the broader picture at continental scales, these studies cannot yet adequately resolve the natural variability of water resources at the HP catchment scale or in mountainous regions in general [9]. Accordingly, the impact of climate warming on HP in snow- and glacier influenced regions still essentially relies on individual case studies [namely from the Alps and US, see, 9], with some regional analyses of the effect of climate warming on snow- and glacier influenced HP available for the US [10,11]. Glacier retreat has in this context long been recognized as potential threat to HP around the world [12–14]. Studies quantifying the actual impact of glacier mass loss on HP are, however, extremely rare. Existing impact studies in the Alpine region focus on the quantification of water resources regime changes [15,16] rather than on quantifying the impact of actual glacier mass loss on hydropower production, as for example in the work of Vergara et al. [17] for the tropical Andes. They showed that glacier retreat might reduce HP for the Cañon del Pato HP plant on the Rio Santa by 570 GWh yr^{-1} if the glacier contribution disappears.

* Corresponding author. UNIL, FGSE-IDYST, Bâtiment Géopolis, 1015, Lausanne, Switzerland.
E-mail address: bettina.schaefli@unil.ch (B. Schaefli).

https://doi.org/10.1016/j.renene.2018.07.104
0960-1481/© 2018 Elsevier Ltd. All rights reserved.

This paper provides, to our knowledge, the first quantification of how HP in an Alpine country, Switzerland, depends on annual glacier mass loss, in the past as well as in the future. The relevance of this study is twofold: i) Swiss HP helps balancing the regional electricity exchanges between France, Germany, Italy and Austria (voltage regulation), guarantees power and frequency modulation (primary, secondary and tertiary controls) and allows for black-start of the regional grid [18]; ii) Swiss HP can be seen as a reference case for all other Alpine HP regions in Austria, Italy and France namely. The methodology used in this paper is also transferable to northern countries with glacier-influenced HP.

Hydropower represents around 55% of the Swiss electricity production, which in 2015 was 61.6 TWh [19]. All large Swiss rivers and many smaller rivers used for HP are influenced by melt water from seasonal snow cover and glaciers. To understand the role of glacier retreat for HP, the key variable is the amount of water that originated from annual glacier mass loss. This number is usually unknown but can be estimated based on observations of the key water balance components, i.e. precipitation and streamflow (Section 3). The recent work of Fischer et al. [20] – who estimated annual mass changes for all glaciers in Switzerland during 1980–2010 – represents a unique opportunity to obtain insights into the role of glaciers for the Swiss water resources.

In this paper, we combine the above estimates with Swiss-wide data for water resources [21], glacier runoff simulations [22] and the spatial database on Swiss hydropower plants developed by Balmer [23] to quantify the role of glaciers for HP in Switzerland. By doing so, we provide the first quantitative assessment for the share of HP that can be attributed to annual glacier mass loss and how this share might evolve in the future owing to changes in water availability from glacier melt. The remainder is organized as follows: we first give an overview over the Swiss HP system (Section 2) and the used data sets (Section 3), before presenting the methods to quantify HP from glacier water resources (Section 4) and the obtained results (Section 5). A detailed discussion of the results (Section 6) and conclusions (Section 7) complete this document.

2. Swiss water resources and HP

The average available water for Switzerland (total water volume divided by area) over the 20th century was around 1300 mm yr^{-1} [24]. Recent estimates of glacier mass change for all Swiss glaciers indicate a net change between 1980 and 2010 of −620 mm yr^{-1} (relative to the glacier area in 2010, i.e. 944 km^2) [20]. This corresponds to −14 mm yr^{-1} when averaged over the area of Switzerland. This negative glacier mass change represents a water input for hydropower production that does not originate from this year's rainfall but from water accumulated decades to centuries ago.

2.1. Hydrological regimes

The temporal distribution of streamflow, or the streamflow regime, is key to understand the interplay of glacier melt water and HP. The streamflow regimes of Switzerland (Fig. 1) are of two fundamentally different types [25,26]: (i) snow- or glacier-dominated regimes that show a pronounced low flow during winter (due to the freezing conditions) and much higher flows during the melt months (April–August), and (ii) rainfall-dominated regimes, where streamflow follows the seasonality of rainfall and of evapotranspiration (resulting in typical summer low flows). An overview of the spatial distribution of streamflow amounts is given in the Supplementary Material (Figure S1).

With anticipated atmospheric warming over the coming decades, major changes in the streamflow regime of snow- and glacier-fed drainage basins are expected [4]. As glaciers retreat, they release water from long-term storage, contributing thereby to a transient increase in annual streamflow for a few decades [27]. The timing of maximum glacier melt volumes depends on the characteristics (elevation range, ice volume) of the catchment and the rate of climate change [28]. In mountainous catchments, significant shifts in the hydrological regime are expected with increasing streamflow in spring and early summer and declining streamflow in July and August [29–31]. These changes result from an earlier onset of the snow melting season and from shrinking glacier areas.

2.2. Swiss hydropower infrastructure

The Swiss HP infrastructure in the year 2016 was composed of 662 powerhouses [32] and 195 large dams that are under the direct supervision of the Swiss federal government [33]. The average annual HP was 35.7 TWh yr^{-1} for the period 1980–2016 (Table 1). The spatial distribution of the HP schemes is conditioned by the discussed specificities of the Swiss hydrological regimes (Fig. 2): the southern and central mountain regions host most of the storage HP schemes; the large run-of-the-river (RoR) schemes are located on the lowland rivers.

The Swiss HP infrastructure can be divided into three main groups [34] (Fig. 2). *Group 1* includes **large storage schemes** that shift large amounts of melt water inflows from summer to winter to

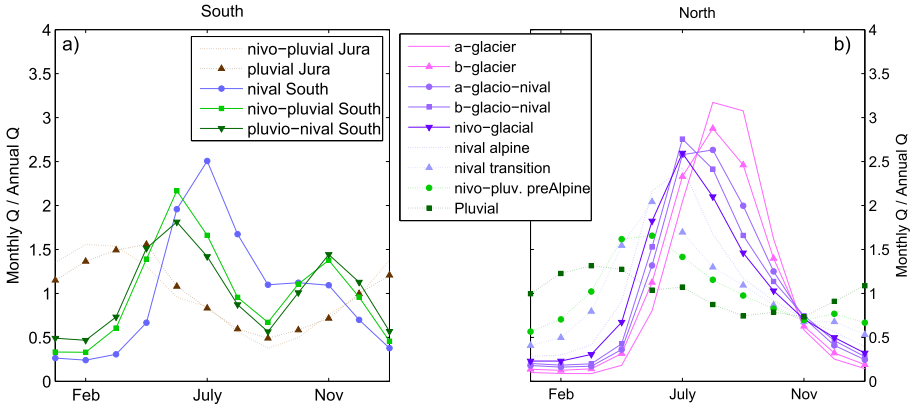

Fig. 1. Swiss hydrological regimes in terms of the ratio between mean monthly streamflow and the mean annual streamflow (denoted as *Q*); a) for south of the Alps and the Jura, b) for north of the Alps. Data source: [57].

Table 1
Overview of Swiss annual hydropower production (1980–2016), including energy consumption for water pumping from lower to upper reservoirs [48].

Hydropower production	TWh yr^{-1}
Average production	35.7
Maximum (year 2001)	42.3
Minimum (year 1996)	29.7
Standard deviation	3.0
Average consumption for pumping	1.9

buffer winter droughts. The group mostly consists of high-head (>100 m) storage schemes with one or several reservoirs (e.g. the well-known Grande Dixence with its storage reservoir of 401,10^6 m^3). These reservoirs have typically natural catchment areas of between 50 and 150 km^2 and waterways draining water from additional, distant catchments. Most group 1 schemes show periods in which their reservoir is full and during which they are operated as run-of-the-river schemes.

Group 2 includes **low-head** (a few tens of meters) **RoR schemes with large catchments** (>2500 km^2) with a typical installed capacity between 5 MW and 100 MW, built on large lowland rivers close to urban and industrial areas. The hydrologic regime of these rivers is strongly influenced by artificial or natural lakes and water management upstream.

Group 3 includes both low-head and high-head **RoR schemes with catchments < 2500 km^2**. Contrary to low-head schemes, **high-head RoR schemes** (with heads from 100 to 1100 m) by-pass a given river-reach and usually have installed capacity below 30 MW. Schemes of group 2 and 3 usually have marginal storage capacity.

A special case are pumped-storage HP schemes that operate between one or two in-stream reservoirs (semi-open or open-loop pumped-storage). The number of such schemes might increase in the near future as a means for grid regulation [35]. They are not discussed separately here. It is noteworthy that both Group 1 and 3 include schemes that transfer water across the natural boarders of the major European rivers (e.g. the Gries HP scheme from the Rhone to the Po basin, the Hongrin scheme from Rhine to Rhone or the Totensee scheme from Rhone to Rhine).

2.3. Climate change impact projections on HP

Numerous studies quantified the effect of climate change on Swiss HP with a so-called climate change impact modeling chain [9]. These studies have a strong focus on high Alpine HP [28,30,36,37]. Only few studies exist on HP in lowland rivers [for an example, see, 26, 38]. While the earliest studies [16,29] made very rough assumptions about the evolution of glacierized surfaces, recent work highlighted the importance of more detailed parameterizations of glacier surface evolution [39] and of reliable estimates of initial ice volumes [40].

The latest comprehensive analysis of climate change impact on Swiss HP was elaborated in the context of two research projects, CCHydro funded by the Swiss Federal Office for the Environment [41] and CCWasserkraft [42] funded by Swisselectric research and the Federal Office for Energy. In agreement with all previous results, these analyses of 50 representative Swiss catchments for the periods 2021–2050 and 2070–2099 concluded that the ongoing warming in the Alps will significantly decrease both the snow cover duration at all altitudes and the maximum annual snow accumulation at high elevations. As a result, Swiss glaciers will strongly reduce in surface by 2100. The combined effect of a reduced snowfall-to-rainfall ratio and of warmer spring temperatures will

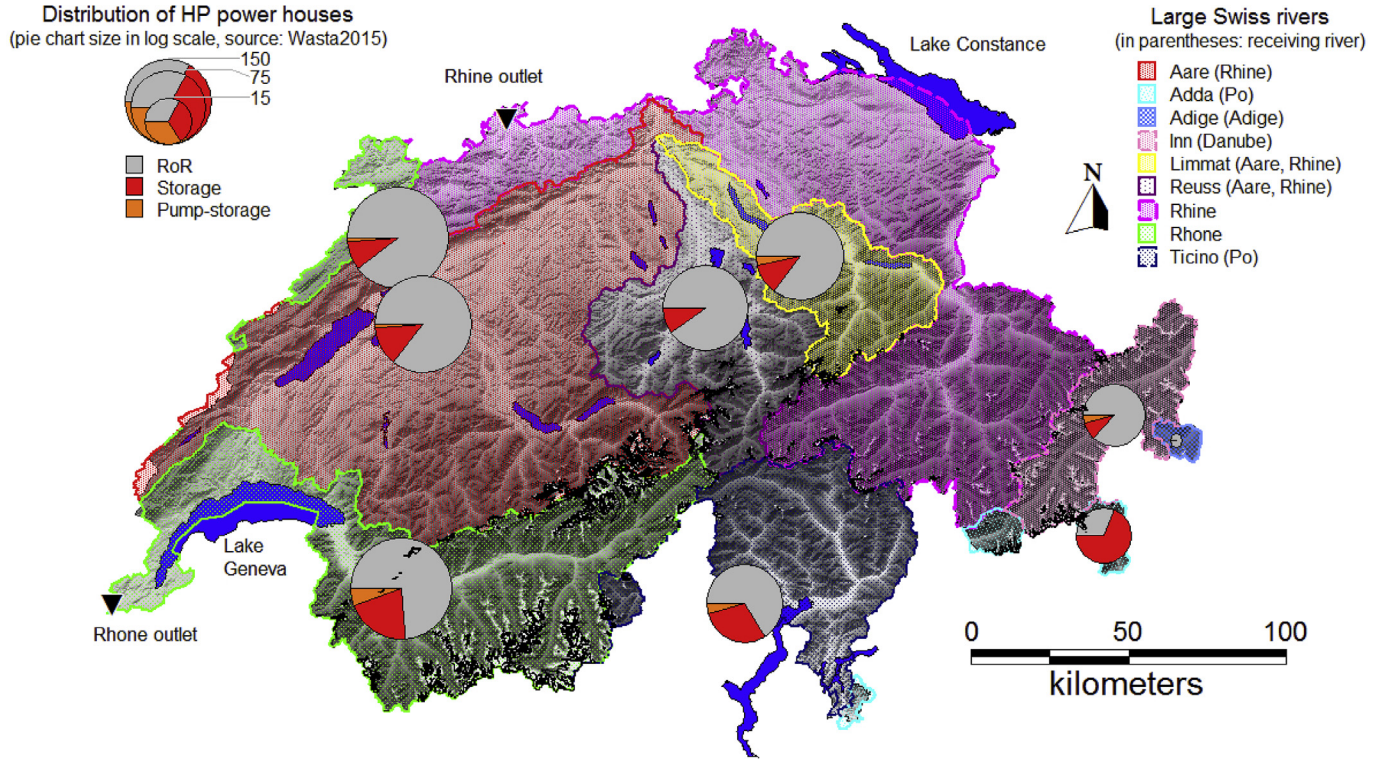

Fig. 2. Distribution of main types of HP powerhouses according to the nine main Swiss river catchments; the Limmat and Reuss feed into the Aare river, which itself feeds into the Rhine river; own representation based on the HP powerhouse type and feeding catchment contained in [WASTA [58]]; other data sources: glacier outline [51], digital elevation model [59], lake vector data: [60], catchment vector data: Swiss Hydrological Atlas HADES [61].

shift the annual maximum monthly streamflow of snow-dominated rivers to earlier periods in the year (up to several weeks). At the same time the snowmelt induced high flows might be more concentrated in time. The concomitant glacier melt will result in a temporary increase of annual streamflow but ultimately lead to reduced annual flows in glacier-influenced catchments, with reduced flows in late summer [43].

In general, late summer streamflow will be reduced in all snow-influenced catchments due to the earlier melting season. For non-glacierized catchments, the annual flow might slightly decrease by 2100 due to a warming-related increase of evapotranspiration and a potential (small) decrease of precipitation. For a comprehensive overview of projected changes, see the work of Speich et al. [44].

The amplitude of changes remains, however, highly uncertain due to uncertainties in both modeling and initial ice volume [45]. An assessment of the volumes of all Swiss glaciers with ground-penetrating radar [46] is ongoing in the context of research for the Swiss energy transition [47].

3. Data sets

The detailed analysis of the role of glaciers for HP is based on five data sets: (i) a GIS database of the Swiss HP infrastructure [HYDROGIS, 23], (ii) the Swiss hydropower production statistics [48], (iii) monthly natural streamflows of the Swiss river network [49], (iv) estimated glacier mass changes between 1980 and 2010 [20], and (v) simulated past and future glacier runoff for all individual Swiss glaciers [22].

3.1. Hydropower infrastructure: HYDROGIS

The GIS data base developed by Balmer [23] includes 401 powerhouses corresponding to a total installed power of 14.5 GW out of the total of 15.0 GW installed in 2005. In 2016, the total installed power was 16.2 GW. During the same time, the total expected production increased from 38.7 GWh to 39.9 GWh [48].

In HYDROGIS, the powerhouses are characterized by their production type (RoR, storage or pump-storage) and for most of them, the installed power and the turbine design discharge are known. Information on the feeding catchments is, however, not available at the powerhouse level since the 401 powerhouses are grouped into 284 HP schemes, which is the reference level for HP catchment information. The database includes furthermore 214 HP reservoirs, 119 dams and 787 water intakes.

For the present analysis, the most important added value of HYDROGIS is the connection between HP schemes and catchments, which was compiled by Balmer [23] via a detailed analysis of adduction tunnels and of company reports of all schemes. Detailed checks showed that the database is reliable in terms of connections between catchments and HP schemes, which is the basis for the water resources analysis herein.

3.2. Hydropower production statistics

Hydropower production statistics are available from the yearly electricity statistics of Switzerland [19] aggregated to six large regions: (i) Ticino, (ii) Grisons, (iii) Valais, (iv) Northern Alps, (iv) Jura, (vi) Plateau (for the correspondence of these regions to main Swiss river catchments see Table S1). Besides actual annual production, the statistics contain annual production potentials, which have to be reported by HP companies for water tax purposes. The production potential is used here as an estimate of the total annual amount of water that was available for production in the catchments (whether used or not).

3.3. Natural streamflow of Swiss rivers

The Swiss Federal Office for the Environment (FOEN) [50] provides a Swiss-wide raster data set (500 m × 500 m) with simulated monthly natural streamflows. This data has been shown to give relatively unbiased estimates of the monthly flows if aggregated to areas between 10 km^2–1000 km^2 (beyond this scale, large lakes might bias the results) [21]. We use here the latest version of the data, made available by Zappa et al. [49]. It covers the period 1981–2000, which thus serves as reference period for all presented analyses.

3.4. Mass changes of Swiss glaciers

Geodetic mass changes between 1980 and 2010 are available for all glacier-covered HP catchments from Fischer et al. (2015). Corresponding glacier outlines are taken from the Swiss Glacier Inventory SGI2010 [51].

Between 1980 and 2010, the estimated average geodetic mass balance for the entire Swiss Alps was −620 mm water equivalent (w.e.) yr^{-1}, with remarkable regional differences (Table 4).

3.5. Glacier runoff

For each individual glacier, past and future glacier mass balance, surface geometry change and retreat, and monthly runoff is available from the Global Glacier Evolution Model (GloGEM, Huss and Hock, 2015). The model has been forced with ERA-interim climate re-analysis data [52] for the past and with 14 Global Circulation Models and three different CO_2-emission pathways [53] until 2100. For the purpose of the present paper, we define glacier runoff as all water exiting the glacier during one month (for details, see the

Table 2
Properties of the electricity statistics regions, including the coefficient of variation (cv) of precipitation and the production potential; glacier cover indicates the relative *glacier cover* for the reference year 2010. The average values for the HP catchments are computed as the average of all scheme catchments of a region. The electricity coefficient is the average value of all powerhouses within a region. Production potential and precipitation data refer to period 1983–2014; normalization with the mean over this period.

Region	Total HP catchment area (km^2)	Joint area (km^2)	# power-houses	Average glacier cover of HP catchments (%)	Average elevation of HP catchments (m asl.)	Average elevation of powerhouses (m asl.)	Normalized annual production potential [min, max]	cv production potential	cv precipi-tation
Switzerland (CH)	39741	528278	402	3.7	1742	752	(0.85, 1.20)	0.08	0.10
Grisons	7088	10235	58	2.0	2162	1014	(0.77, 1.41)	0.14	0.10
Valais	5200	27324	70	12.2	2414	773	(0.83, 1.16)	0.07	0.10
Ticino	2735	2357	33	0.2	1816	1010	(0.63, 1.36)	0.16	0.11
Jura	2532	7075	8	0.0	992	637	(0.68, 1.36)	0.15	0.11
Plateau	10037	234419	147	1.3	1124	482	(0.87, 1.14)	0.07	0.11
North Alps	12408	246868	86	2.3	1530	658	(0.86, 1.15)	0.06	0.12

Table 3
Characteristic electricity coefficients (EC), computed at different levels. Area-scale ECs express how much hydropower is produced per m^3 of water originating in that area, point -scale ECs express how much hydropower is produced per m^3 transiting through that point. The weighing type indicates how the underlying data is weighed (*design discharge* is the design discharge of the turbines, *exp*. stands for *expected* and designates a design value rather than an actual observed value.

EC name	Scale	Aggregation level	Underlying EC data	Weighing	kWh m^{-3}
Powerhouses, average (n = 284)	Point-scale	Powerhouses	Powerhouses	No weighing	0.634
Powerhouses, max	Point-scale	Powerhouses	Powerhouses	Does not apply	4.444
Powerhouses, min	Point-scale	Powerhouses	Powerhouses	Does not apply	0.004
Schemes, average	Area-scale	Schemes	Powerhouses	Exp. production hours x design discharge	0.591
Grisons	Area-scale	Production region	Schemes	Exp. annual production	0.856
Valais	Area-scale	Production region	Schemes	Exp. annual production	1.707
Ticino	Area-scale	Production region	Schemes	Exp. annual production	0.997
Jura	Area-scale	Production region	Schemes	Exp. annual production	0.216
Plateau	Area-scale	Production region	Schemes	Exp. annual production	0.020
North Alps	Area-scale	Production region	Schemes	Exp. annual production	0.530
Switzerland	Area-scale	Switzerland	Schemes	Exp. annual production	0.906
Rhine	Point-scale	HP Network	Powerhouses	Exp. production hours x design discharge	0.041
Rhine outlet, Birsfelden	Point-scale	Scheme	Powerhouses	Does not apply	0.018
Rhone	Point-scale	HP Network	Powerhouses	Exp. production hours x design discharge	0.269
Rhone outlet, Chancy-Pougny	Point-scale	Scheme	Powerhouses	Does not apply	0.021
CH glacier area	Area-scale	Switzerland	Regions	Interpolated from regions	2.101
Rhine glacier area	Area-scale	Switzerland	Regions	Interpolated from regions	1.892
Rhone glacier area	Area-scale	Switzerland	Regions	Interpolated from regions	2.212

Table 4
Observed average glacier mass balance changes (in mm of water equivalent) for Switzerland (CH), the Rhine and the Rhone HP catchments at their outlet and the corresponding ratio of net annual ice melt to average annual discharge without considering HP nesting. A few glaciers are not included neither in the Rhine river HP network nor in the Rhone HP network; some glacier water of the physiographic Rhone catchment is exported, i.e. does not feed the Rhone river HP network (e.g. Gries).

	Area HP production catchments (km^2)	Annual glacier Mass loss (mm yr^{-1})		Glacier area (km^2)		Avg discharge reference period (mm yr^{-1})		Ratio of annual glacier mass loss to discharge (%)	
		1981–2000	1980–2010	1973	2010	1981–2000	1980–2010	1981–2000	1980–2010
CH	39741	479	620	1261.2	942.8	1037	1013	1.3	1.7
Rhine	26520	502	634	406.3	283.0	1007	984	0.65	0.8
Rhone	7655	452	579	682.5	543.4	1109	1092	3.3	4.2

Supplementary Material).

The future glacier runoff simulations from GloGEM show the expected decrease of glacier runoff in the period 2040–2060 for catchments with low glacier coverage. For the period 2070–2090, the simulations show a consistent decrease of glacier runoff for all HP catchments [Figure S2 and [43]].

4. Methods

We give hereafter details on how HP is estimated at different scales based on discharge data for different time periods, followed by details on the assessment of past and future HP from annual glacier mass loss and of expected HP changes resulting from hydrologic regime modifications.

4.1. Estimation of HP production at the scheme scale

The HP data available at the powerhouse level includes the expected annual electricity production for average years (based on past operation), E_h^* [Wh yr^{-1}], the total available power, P_h^* [W], and the total design discharge through the turbines, Q_h^* [m^3 s^{-1}], where h designates the (power)house level. A first order estimate of the number of powerhouse operating hours, τ_h^* [h yr^{-1}], can thus be obtained as:

$$\tau_h^* = \frac{E_h^*}{P_h^*}. \quad (1)$$

The asterisk (*) is used to identify design variables and not actual time-varying quantities. Note that the estimate neglects the percentage of time that only part of the powerhouse capacity is used (i.e. not all turbines in use or at partial load).

Based on τ_h^*, we estimate a first lumped water-to-electricity conversion factor, called electricity coefficient, γ_h^* [kWh m^{-3}] as follows:

$$\gamma_h^* = \frac{E_h^*}{Q_h^* \tau_h^* 3600 \cdot 10^3} = \frac{P_h^*}{Q_h^* 3600 \cdot 10^3}. \quad (2)$$

The electricity coefficients obtained at the scale of the powerhouses, γ_h^*, can be summed up to the scale of the HP schemes:

$$\gamma_j^* = \sum_{\forall h \in j} \gamma_h^*, \quad (3)$$

where γ_j^* is the electricity coefficient of scheme j.

This electricity coefficient γ_j^* relates indirectly the average annual streamflow available from the catchment Q_j [m^3 s^{-1}] to the corresponding electricity production at the scheme level, based on the past average electricity production. However, not all powerhouses within a catchment use the water of the entire catchment and the catchments corresponding to each powerhouse are unknown. We thus assume that the design discharge for each powerhouse, Q_h^*, multiplied by the expected operation hours, τ_h^*, is representative of the amount of annual water that feeds this powerhouse. This assumption is adequate for storage plants, which mostly operate in design conditions. For RoR schemes this assumption leads to underestimating the operation hours and overestimating the electricity coefficient.

Accordingly, we propose to use the following weighted scheme-scale electricity coefficient $\hat{\gamma}_j$:

$$\widehat{\gamma_j} = \frac{\sum_{\forall h \in j} E_h^*}{3600 \sum_{\forall h \in j} Q_h^* \tau_h^*} = \frac{\sum_{\forall h \in j} \gamma_h^* Q_h^* \tau_h^*}{\sum_{\forall h \in j} Q_h^* \tau_h^*}, \quad (4)$$

Actual discharge time series for different time periods are available at the catchment-scale only. An estimate of the discharge Q_{hi} feeding each powerhouse h over time period i is obtained as:

$$Q_{hi} = Q_{ij} \frac{Q_h^*}{\sum_{\forall h \in j} Q_h^*}, \quad (5)$$

where Q_{ij} [$m^3\ s^{-1}$] is the average annual discharge available for the scheme catchment j during time period i.

The weighted scheme-scale electricity coefficient is the key to estimate HP from annual glacier mass loss for past and future time periods at the scheme-scale.

4.2. Estimation of HP production at the regional scale

The electricity statistics also report production statistics for six regions of Switzerland. To obtain a regional-scale electricity coefficient $\widehat{\gamma_r}$ [kWh m^{-3}] for region r, the scheme-scale electricity coefficients are weighted according to their expected total production (a flow-time scaling is not possible since the concept of operating hours does not make sense at the scheme scale):

$$\widehat{\gamma_r} = \frac{\sum_{\forall j \in r} \widehat{\gamma_j} E_j^*}{\sum_{\forall j \in r} E_j^*}. \quad (6)$$

Where $E_j^* = \sum_{\forall h \in j} E_h^*$ is the expected production at the scheme level. This regional-scale electricity coefficient expresses how much hydropower is produced from a m^3 of water flow that is originating in that region.

4.3. Estimation of HP production at the HP network scale

Changing the perspective from the hydropower producing catchment to a hydropower producing river reach, we can estimate a weighted electricity coefficient $\widehat{\gamma_x}$ at a given location x:

$$\widehat{\gamma_x} = \frac{\sum_{\forall h \text{ upstream } x} E_h^*}{3600 \sum_{\forall h \text{ upstream } x} Q_h^* \tau_h^*} = \frac{\sum_{\forall h \text{ upstream } x} \gamma_h^* Q_h^* \tau_h^*}{\sum_{\forall h \text{ upstream } x} Q_h^* \tau_h^*}. \quad (7)$$

While $\widehat{\gamma_j}$ expresses how much hydropower is produced from a m^3 of water flow generated in a catchment, this point-scale electricity coefficient, $\widehat{\gamma_x}$, expresses how much electricity is generated per m^3 of water that transits a given location x in a river.

The total hydropower production of the entire HP network upstream of location x for period i is then obtained as:

$$E_{ix} = 3600 \cdot 10^3 \sum_{\forall h \text{ upstream } x} \gamma_h^* Q_{ih} \tau_h^*. \quad (8)$$

4.4. Analysis of past and future water resources availability from annual glacier mass loss

Based on the observed data of Fischer et al. [20,51], we propose to estimate the share of water resources that results from glacier mass depletion, ρ_{ij}, at the scale of all HP scheme catchments as follows:

$$\rho_{ij} = \frac{m_{ij}}{q_{ij}}, \quad (9)$$

where m_{ij} [mm yr^{-1}] is the average annual glacier mass loss in catchment j over period i, and q_{ij} [mm yr^{-1}] is the specific discharge of catchment j (discharge in $m^3\ s^{-1}$ divided by the catchment area). Given the assumed linear relationship between annual HP, $E_{ij,}$ and available discharge (Equation (7)), ρ_{ij} gives a direct estimate of the share of annual HP that results from glacier mass depletion.

Discharge and ice melt data are available for the following periods: $T_{ref} = 1981–2000$, $T_1 = 2040–2060$ and $T_2 = 2070–2090$. In addition, some results are reported for the time period 1980–2010, which is the original reference period for the mass balance data published by Fischer et al. [20].

4.5. Future regime impacts on HP

Climate change induced modifications of glacier runoff affect the water availability in terms of quantity and temporal occurrence (an example of future simulated glacier runoff is given in Fig. 3). We quantify the effect of regime modifications on HP in terms of the absolute difference of the runoff volume from the glacier-covered area between two time periods for each month m:

$$V_{ij}^g(m) = \left| Q_{ij}^g(m) - Q_{\text{ref},j}^g(m) \right| \Delta_m, \quad (10)$$

where $V_{ij}^g(m)$ [m^3] is the glacier (g) runoff volume difference for month m, time period i and catchment j, $Q_{ij}^g(m)$ [$m^3\ s^{-1}$] is the monthly simulated glacier runoff of time period i, and $Q_{\text{ref},j}^g(m)$ [$m^3 s^{-1}$] is the monthly glacier runoff for the reference period. Δ_m [s] is the duration of the month. The reference area for V_{ij}^g, Q_{ij}^g, and $Q_{\text{ref},j}^g$ is the glacier-covered area during the reference period. For future periods, in which glaciers have retreated, this area will notably include ice-free surfaces as well.

A glacier runoff change indicator δ_{ij} is obtained by (i) normalizing $V_{ij}^g(m)$to the total catchment discharge $Q_{\text{ref},j}(m)$ for the reference period and (ii) averaging over all months (see Figure S3 for an illustration):

$$\delta_{ij} = \sum_{m=1}^{12} \frac{V_{ij}(m)}{Q_{\text{ref},j}(m) \Delta_m}. \quad (11)$$

δ_{ij} is the relative amount of water that, for period i, is available during a different period of the year than it was for the reference period. Assuming again a linear relationship between annual HP and available discharge, δ_{ij} can also be directly interpreted in terms of HP: it gives the relative amount of annual HP that, in the future, will be available during a different period of the year.

5. Results

5.1. Swiss HP overview

The Swiss HP schemes use the water of an area of 39,740 km^2, corresponding to 93% of the Swiss territory and including all Swiss glaciers. The large percentage is due to the run-of-river (RoR) HP schemes in series on all large rivers leaving Switzerland (Fig. 2 and

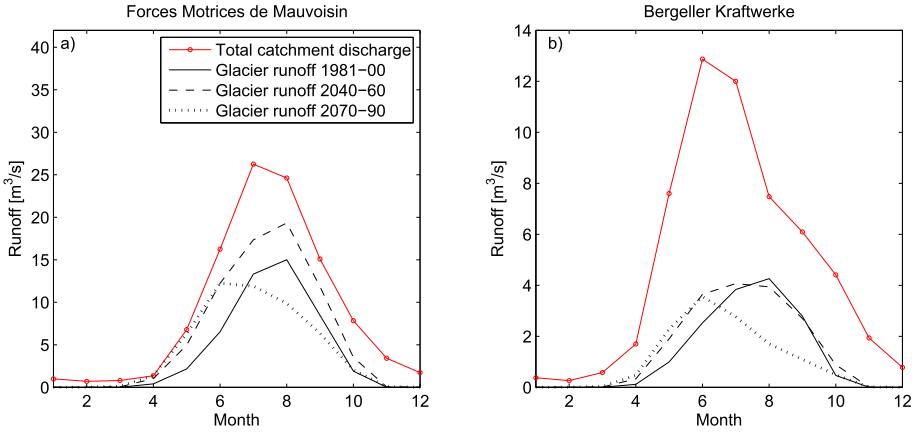

Fig. 3. Present and future glacier runoff compared to the catchment discharge for the reference period for two selected HP catchments: a) Mauvoisin HP scheme located in the Upper Rhone River catchment; b) Bergeller HP scheme located in the Adda catchment (see Fig. 2). Data source: glacier runoff [22], catchment discharge [49].

Table S2). The cumulative sum of all HP scheme catchments amounts to 528,278 km^2 or roughly 13 times the total catchment area (Table 2), which emphasizes the degree of nesting of the HP catchments, in particular in low-lying areas (Plateau region, North of the Alpes region).

On average, the water from the 134 headwater catchments is used in 12 HP stages, with 12 headwater catchments that are not part of a larger HP network. The water from some Alpine headwater catchments is used in up to 30 HP stages down to the Rhine in Basel.

5.2. Natural variability of Swiss HP resources

Measured in terms of production potential, the six major HP regions (Table 2) show important differences in interannual variability of available water (Fig. 4a), with coefficients of variations (standard deviation divided by the mean) ranging from 0.06 to 0.16. The interannual variability of precipitation (Fig. 4b), in contrast, is rather similar across all regions, with a coefficient of variation between 0.10 and 0.11.

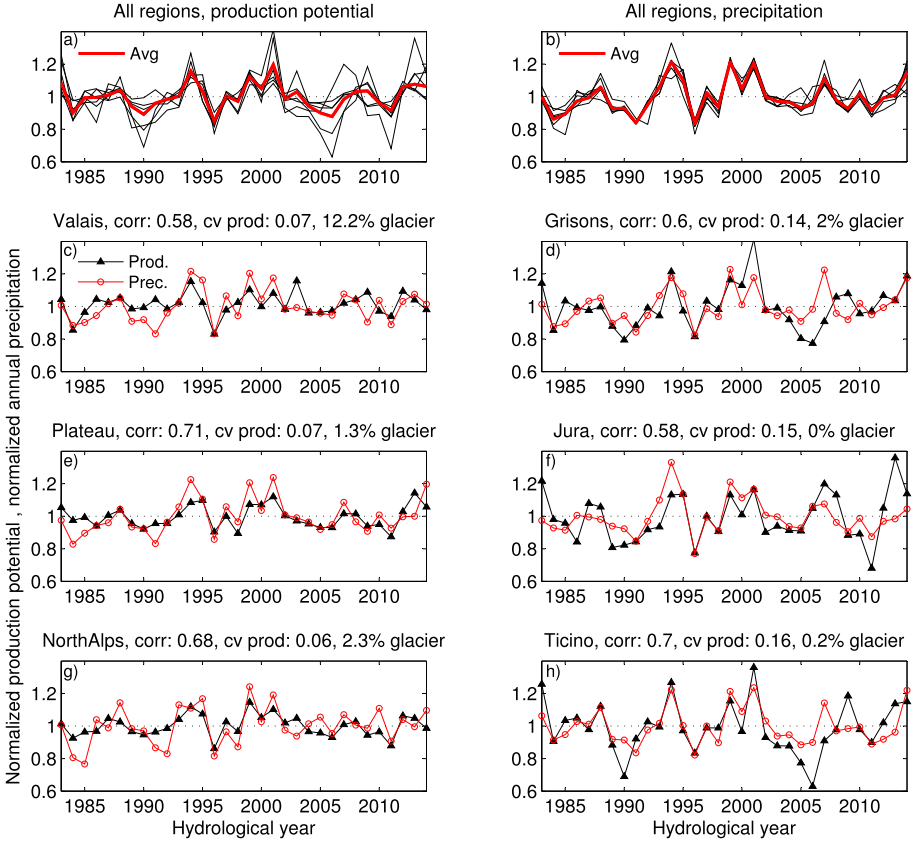
All regions, production potential
All regions, precipitation
Avg
Valais, corr: 0.58, cv prod: 0.07, 12.2% glacier
Grisons, corr: 0.6, cv prod: 0.14, 2% glacier
Plateau, corr: 0.71, cv prod: 0.07, 1.3% glacier
Jura, corr: 0.58, cv prod: 0.15, 0% glacier
NorthAlps, corr: 0.68, cv prod: 0.06, 2.3% glacier
Ticino, corr: 0.7, cv prod: 0.16, 0.2% glacier
Prod.
Prec.
Normalized production potential , normalized annual precipitation
Hydrological year

Fig. 4. Normalized annual production potential and annual precipitation (with reference to the average value for the period 1983–2014): a) production potential for each of the six regions used in the electricity statistics and country-average, b) precipitation for each region and country-average (data as recorded at the SwissMetNet stations [62], c) to h) production potential and precipitation per region; given is also the correlation between production potential and precipitation (*corr*), the coefficient of variation of the production potential (*cv prod*) and the degree of glacier cover. The hydrological year starts on 1 Oct.

The lowest variability of the production potential is obtained for the region with the highest glacierization (Valais, Fig. 4c) and for the Plateau region (Fig. 4e). For the Valais, as for other areas with a high glacierization, the glaciers act as a strong buffer of interannual variability. This notably results in a relatively stable interannual operation of high elevation HP reservoirs across Switzerland [see 26, including an illustration of Swiss reservoir filling curves].

The low variability of the production potential of the Plateau region can be explained by the large number of RoR power plants with large catchments, for which the spatial precipitation variability averages out. At the Swiss scale, the low variability of the production potential results from an averaging effect across regions.

5.3. Electricity coefficients from the scheme scale to the regional scale

Swiss HP infrastructure shows high electricity coefficients, with an average electricity coefficient of the analyzed powerhouses of 0.63 kWh m^{-3} and an average scheme scale electricity coefficient of 0.59 kWh m^{-3} (Table 3). For individual schemes, the values range from 0.004 kWh m^{-3} for lowland RoR schemes to up to 3.84 kWh m^{-3} for the single-stage high-head Cleuson- Dixence HP scheme (Fig. 5 and Fig. 6).

The overall high scheme-scale electricity coefficients are explained by the high electricity coefficients of headwater catchments, with an average of 0.95 kWh m^{-3} (Fig. 5a). Three of these headwater schemes have both a particularly high head with their powerhouses located at low elevation in the Rhone valley bottom and high elevation catchments, resulting in electricity coefficients above 3 kWh m^{-3} (Fig. 5a).

At the level of the electricity statistics regions, a generally strong elevation trend of electricity coefficients becomes visible (Fig. 5b). The trend is of 1.00 kWh m^{-3} per 1000 m of increase of the mean catchment elevation. This Swiss-wide trend can be converted into a rough estimate of the electricity coefficient of HP from glacier melt water: given the mean elevation of the Swiss glaciers by 2010, 3042 m asl), the general elevation trend of regional electricity coefficients (Fig. 5b) yields an electricity coefficient of 1.00 10^{-3} kWh m^{-3} $m^{-1}\times$ 3042 m -0.940 kWh $m^{-3} = 2.11$ kWh m^{-3} (see Section 5.5 for further details).

5.4. Electricity coefficients at the HP network scale

The effect of having sequences of HP schemes along rivers can be illustrated based on the two largest HP networks, the one along the Rhine river and along the Rhone river (Fig. 2). The Rhine HP network has a weighted electricity coefficient of 0.04 kWh m^{-3}, which is twice as high as the electricity coefficient of the hydropower plant operating on the Rhine at its Swiss outlet (Birsfelden), which equals $\gamma_h = 0.02$ kWh m^{-3} (Table 3). For the Rhone catchment, including many high-head hydropower plants and with water being used in up to 9 stages, the weighted electricity coefficient of the entire HP network equals 0.27 kWh m^{-3}, which is more than 10 times the electricity coefficient of the powerhouse on the Rhone at its Swiss outlet (at Chancy-Pougny, 0.02 kWh m^{-3}).

5.5. Estimation of HP production from annual glacier mass loss

The high elevation HP schemes receive a significant amount of water input from annual glacier mass change, up to 500 mm yr^{-1} (relative to the scheme catchment area) for 1981–2000, or more than 25% of the total annual catchment discharge (Fig. 7).

On a Swiss-wide area-average, the glaciers' net contribution was of 479 mm w.e. yr^{-1} for 1981–2000 (Table 4). During this period, the average Swiss glacier cover was 1111 km^2 (assuming a linear retreat of the glacier area between 1973 and 2010) [20]. A first rough estimate of the HP originating from annual glacier mass loss can be obtained with the regional electricity coefficient extrapolated to the mean glacier elevation. The corresponding production over 1981–2000 equals thus 0.479 m $yr^{-1} \times 1111{,}10^6$ $m^2 \times 2.11$ kWh $m^{-3} = 1123$ GWh yr^{-1}, or 3.2% of the Swiss-wide annual production over the same period, which was 34,738 GWh yr^{-1} [48]. For the period 1980–2010, which had a stronger annual glacier mass loss (Table 4), this ratio equals 4.0% (Table 5).

This estimation of HP ratios from glacier mass loss relies on two numbers: the average annual glacier mass loss and the electricity coefficient estimated from design data (expected annual production, production time and turbine flow). The annual glacier mass loss has an uncertainty of ± 0.07 m yr^{-1} [20]. For the interpolated area of individual glaciers between observation dates, an error of $\pm 5\%$ can be assumed as a conservative estimate. The 95% confidence interval of the electricity coefficient interpolated at the Swiss-scale for glaciers (from linear regression analysis) is 2.11 ± 0.68 kWh m^{-3}. Inserting these uncertainties into the above regional estimate of HP from glacier-covered areas results in estimated HP from annual glacier mass loss of between 1.8% and 5.2% for the period 1980 to 2000 and 2.3%–6.2% for the period 1981 to 2010.

HP calculations based on scheme-scale melt ratios (Fig. 8a) gives very similar estimates: the production ratio ρ_{ij} averaged over all glacier schemes, weighted by the expected scheme production,

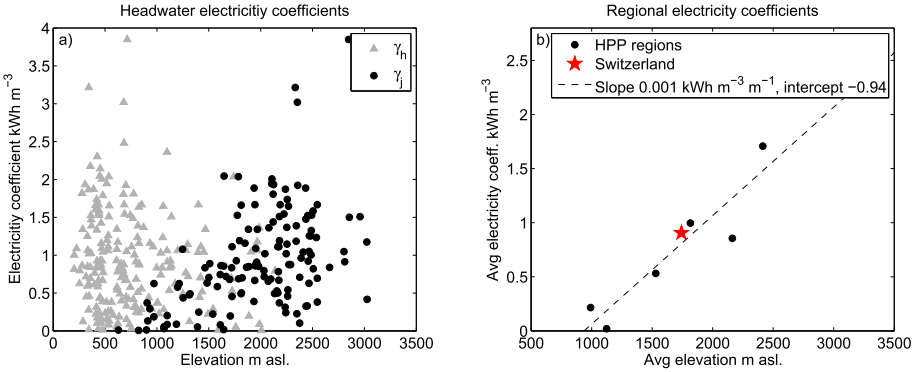

Fig. 5. Relationship between elevation and electricity coefficients: a) electricity coefficients at the scale of headwater catchments; shown are the power house electricity coefficients γ_h against power house elevation and the scheme-scale electricity coefficients $\widehat{\gamma}_j$ against catchment elevation; b) regional electricity coefficients,$\widehat{\gamma}_r$, for the six HP regions and for entire Switzerland against average scheme catchment elevation.

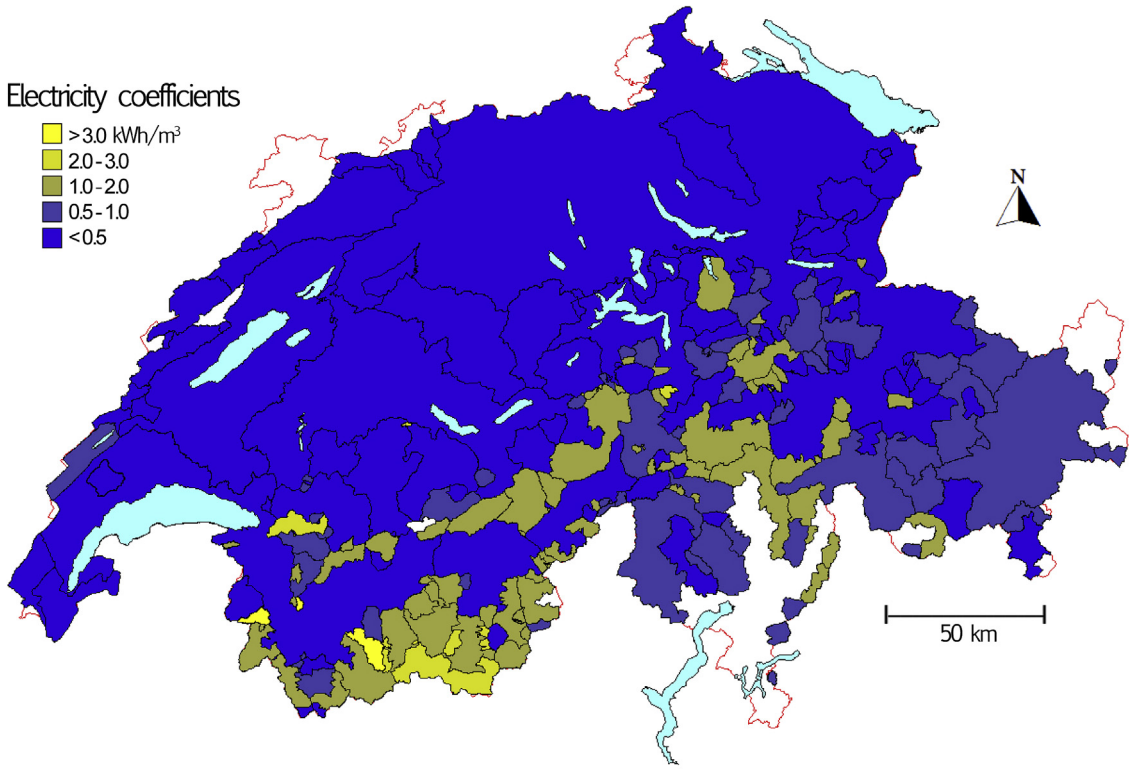

Fig. 6. Spatial distribution of electricity coefficients of all HP schemes. The catchments are nested, lowland RoR catchments contain upstream catchments. Light blue corresponds to lake areas.

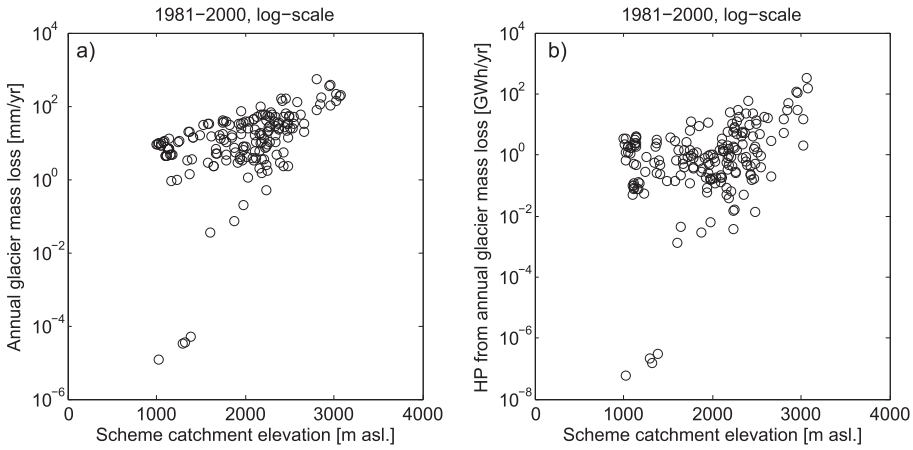

Fig. 7. Annual glacier mass loss and corresponding hydropower production as a function of scheme catchment elevation for the period 1981–2000; a) annual glacier mass loss in mm yr^{-1} (log-scale) b) estimated hydropower production from annual glacier mass loss (multiplied with the electricity coefficient $\hat{\gamma}_r$) in GWh yr^{-1}.

equals 3.2% for the period 1981–2000 and 4.0% for 1980–2010 (Table 5). These Swiss-wide averages of HP production ratios from glacier mass loss hide significant regional differences, with estimates for the past periods ranging from between 6.4 and 7.8% for the Rhone river to between 1.8% and 2.2% for the Rhine river (Table 5).

For the future, the GloGEM simulations predict that 55% and 79% of the 2010 glacier volume will be lost by 2040–2060 and 2070–2090, respectively (Table S3). The strong reduction from 2010 to 2040–2060 is coherent with the observed loss of 37% (22.5 km^3) over the period 1980–2010 (the estimated glacier volume for 2010 was of 59.9 km^3; [20]. The corresponding simulated annual glacier mass loss rates at the scheme-scale result in an average ρ_{ij}, of 2.5% for 2040–2060 (Fig. 8c) and of 1.2% for 2070–2090 (average over glacier schemes, (Table 5).

The maps of ρ_{ij} (Fig. 8c and d) reveal that, in the past, annual glacier mass loss was an important source of water for HP at larger scales and not only in the headwater catchments. Given the strong glacier retreat, the input from annual glacier mass loss is, however, significantly reduced in future simulations. For the Rhine river, input from annual glacier mass loss is likely to become insignificant in the future (Table 5).

For the Rhone river catchment, the simulations suggest that the decrease in HP from annual glacier mass loss might only occur after

Table 5
Estimated average HP ratios from glacier melt, $\bar{\rho}_{CH}$, estimated either from ratios of net glacier melt to total discharge (labeled discharge ratios) or from glacier-averaged electricity coefficient (see Table 3), labeled EC. Confidence limits (given in brackets) can be calculated for the EC method only; discharge-based estimations are weighted averages over the schemes, with weights corresponding to the expected annual production of each scheme. For the simulations, the net ice melt corresponds to the melt between two simulation time periods.

Estimation method	Reference period simulation	Period	Source	$\bar{\rho}_{CH}$ (−)	$\bar{\rho}_{Rhone}$ (−)	$\bar{\rho}_{Rhine}$ (−)
avg EC		1981–2000	Obs	3.2 (1.8,5.2)	6.4 (3.4,10.2)	1.8 (1.0,2.9)
avg EC		1980–2010	Obs	4.0 (2.3,6.2)	7.8 (4.4,12.2)	2.2 (1.3,3.4)
Discharge ratios		1981–2000	Obs	3.1	7.0	1.5
Discharge ratios		1980–2010	Obs	3.8	8.6	1.8
Discharge ratios	2010–2020	2040–2060	GloGEM	2.5	7.1	0.4
Discharge ratios	2040–2060	2070–2090	GloGEM	1.2	3.8	0.1
	Expected production GWh yr^{-1}	2005	HYDROGIS	36458	10341	18931
	Avg HP GWh yr^{-1}	1981–2000	Electricity stat.	34738	9853[a]	18038[a]
	Avg HP GWh yr^{-1}	1980–2010	Electricity stat	35241	9996[a]	18299[a]
	Avg glacier elevation		SwissTopo	3042	3170	2814

[a] Estimated by scaling the Swiss-wide production by the expected production.

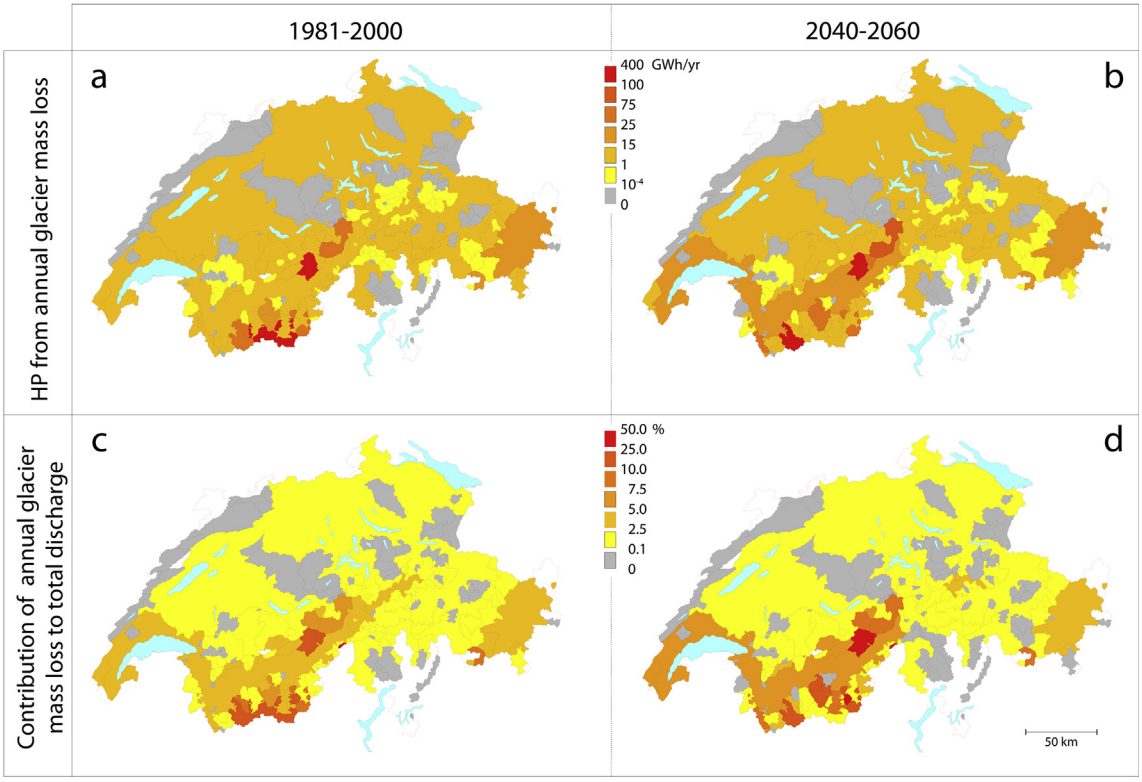

Fig. 8. Spatial distribution of the hydropower production from glacier mass loss; a) hydropower production from glacier mass loss in GWh yr−1 for the period 1981–2010, b) for the period 2040–2060 based on GloGEM simulations, c) ratios ρij for the period 1981–2000, d) ratios for the period 2040–2060 based on GloGEM simulations.

the period 2040–2060. The contributions, however, will remain significant for this century, with 3.8% estimated for the period 2070–2090 (Table 5).

5.6. Impacts of glacier runoff regime changes

Future runoff from glacier catchments is, on average, expected to shift to earlier periods in the year, especially for catchments with important glacier volume loss. The simulated glacier runoff shifts, as summarized by the indicator δ_{ij}, correspond mostly to less than 10% of the scheme-scale discharges. This is true for both periods 2040–2060 and 2070–2090 (Fig. 9). The notable exception are a few run-of-river schemes that are located at elevations higher than 1400 m asl. Here, shifts go up to 35% for the period 2040–2060. Given the strong simulated glacier retreat up to then, the regimes shift only slightly beyond this period.

6. Discussion

The method proposed in this paper to analyze the impact of glacier retreat on HP brings together a number of data sets that have not been analyzed jointly so far. In particular, it combines recent model results on glacier mass evolution, estimates for glacier runoff and catchment-scale river discharge, as well as statistics and spatial information on hydropower infrastructure. The contribution of annual glacier mass change to HP is estimated in two different ways: either (a) by estimating and averaging ratios of annual glacier mass loss and total discharge for all HP scheme catchments, or (b) from an elevation-dependent electricity production factor and the mean glacier elevation. Whilst the first

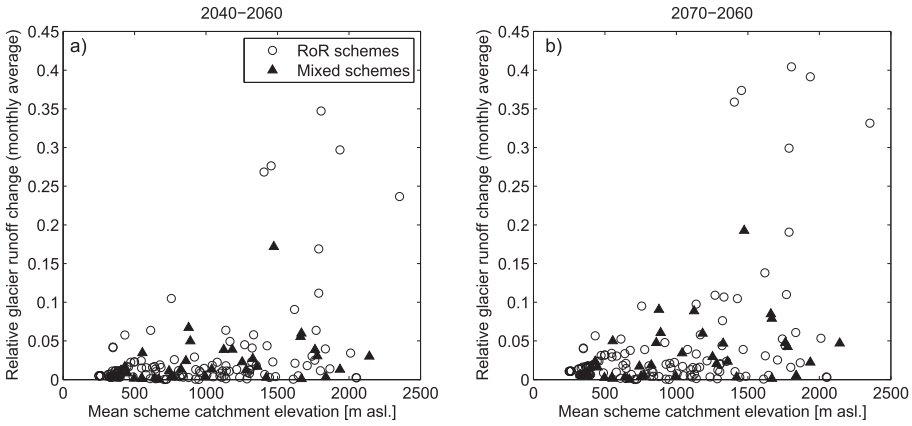

Fig. 9. Glacier runoff change ratios (δ_{ij}) for all schemes that had glaciers during the reference period, plotted against scheme catchment elevation: left, period 2040–2060; right, period 2070–2090. The reference period is 1981–2000 for both future periods. Mixed schemes have run-of-river (RoR) and (pump-)storage hydropower production.

method relies on discharge estimates that are based on simulations and observations, the second only relies on observed glacier mass balance data and interpolated electricity coefficients.

Both methods give similar results for the share of HP resulting from the depletion of glacier mass, with Swiss-wide average estimates ranging from 3.1% to 4.0% for the observation periods. The relevance of this result is twofold: i) In terms of transferability of the proposed method, the obtained results suggest that similar analyses could be completed in any region that has detailed glacier mass balance data and spatial information on electricity coefficients. ii) For Switzerland, the estimated ratios give a robust estimate of the amount of Swiss-wide HP that originated from annual glacier mass loss in the recent past. It has to be noted that these numbers are considerably higher than the simple average share (not weighted by production) of water originating from glacier mass depletion in the various scheme catchments. The latter, in fact, amounts to only between 1.3% and 1.7% (Table 4). This almost doubling effect between the average ratio of water availability from glacier mass depletion and the corresponding average ratio of HP is a direct consequence of using the glacier melt water several times along the HP network and of the high electricity coefficients associated with glacier water resources.

The simulations suggest that, on a Swiss-wide basis, HP might receive a significantly lower share of water from annual glacier mass loss already in the near future. Compared to 1981–2000, the future simulations predict a reduction of the HP ratios from 3.1% to 2.5% for the period 2040–2060 and to 1.2% for 2070–2090. This corresponds to a production reduction of around 0.56 TWh yr^{-1} for 2040–2060 and of around 1.00 TWh yr^{-1} for 2070–2090.

This share of HP from glacier mass depletion has to be put into relation to other changes expected for HP in the near future. HP is namely expected to decrease by 1.4 TWh yr^{-1} due to the implementation of the Swiss water protection act during concession renewals [47,54]. This is in contrast to the Swiss Energy Strategy 2050, that plans a net HP increase (beyond water protection effects) by at least 1.5 TWh yr^{-1}. According to the same strategy, this should be obtained by building new small hydropower plants (+1.3 TWh yr^{-1}) and from the extension and adaptation of existing large plants (+0.9 TWh yr^{-1}) [34,47], which is challenging given that all major Swiss river systems are already exploited [34].

The reduction of annual melt water might well be the dominant warming-induced impact for many schemes. The presented analysis shows, however, that for most schemes, the future temporal pattern of glacier melt water inflow will result in a redistribution of less than 10% of the total available water. In other terms, the annual HP pattern will not fundamentally change for those schemes. It must be noted, however, that this does not applies to RoR schemes that have catchments currently exhibiting an important degree of glacier coverage. Such schemes might in fact experience a profound modification of their water inflow regime already in the near future.

Given the individual character of HP schemes, a more detailed analysis of the temporal redistribution of melt water flows is challenging and would require a detailed analysis at the level of water intakes. Some water intakes might e.g. lose water during future melt periods if the melt water flow is more concentrated on shorter periods and thus exceeds the intake capacity (resulting in a potential increase of overspill duration and magnitude). This might in particular affect glacier-influenced storage HP schemes that usually have a high number of water intakes [e.g. the Grande Dixence scheme has 100 km of tunnels to route the water of 75 water intakes to its main reservoir, 55]. The Swiss-wide database on water intakes [which includes 1406 HPP intakes, 56, p. 22] is, however, known to be incomplete and contains essentially the intakes that are directly relevant for residual flows.

A third implication of climate warming for glacier-influenced HP is a potential modification of the year-to-year variability of available water. This modification is anticipated in many climate change impact studies in high Alpine environments [29]. With the average monthly flow data used in this study, no further assessment of this important aspect is possible. However, the analyses presented for the annual hydropower production potential (quantifying the production potential) and for the annual precipitation variability at a regional scale shows that there is no clear link between the today's amounts of glacier cover and the annual variability in the production potential. This result is unexpected since HP regions with a high glacier cover were previously thought to show a relatively low year-to-year variability of hydropower production potential [26]. Understanding in detail how the HP network structure buffers current year-to-year precipitation variability and how this might evolve in the future is left for future research.

7. Conclusion

Alpine hydropower production (HP) is benefitting from glacier water resources that have been accumulated decades and centuries ago, and that cannot be replenished in the near future. This first quantification of the HP share originating from annual glacier mass loss at the scale of an Alpine region reveals that 3.1%–4% of the total annual Swiss HP presently originates from this transient water

resource. The share will rapidly decline for all Swiss regions, resulting in a reduction of the present-day production levels of about 1.0 TWh yr^{-1} by mid-century. This figure is comparable to the 1.4 TWh yr^{-1} production loss that can be expected from the implementation of the new Swiss water protection act [47,54]. An exception is given for the Rhone river catchment, in which the relatively large amount of glaciers will continue to provide increased amounts of melt water at least until the late 2040s.

Despite of observational uncertainties, we have shown that the presented estimates are robust. We anticipate our results to have direct implications for national HP infrastructure projects, such as storage increase at high elevation sites or multipurpose projects combining HP and the regulation of interannual hydrological variability.

Beyond the scale of the analyzed case study, the relevance of our results can be summarized as follows: First of all, the results for Switzerland show that the impact of glacier retreat on HP can be reliably estimated from regional electricity coefficient trends, which here was shown to be of around 1.0 kWh m^{-3} per 1000 m elevation increase. Second, the results for Switzerland underline that significant annual HP reduction might result from glacier retreat already in the near future; the highlighted large regional differences call for more detailed studies in Europe and elsewhere.

Acknowledgements

The first two authors acknowledge the funding by the Swiss Competence Centre for Energy Research – Supply of Electricity (SCCER-SoE, Switzerland). The work of the last author was funded by the Swiss National Science Foundation (SNSF Ambizione Energy grant number 154290). The HydroGIS database was made available by M. Balmer. The meteorological data (ANETZ stations) is available from MeteoSwiss (https://gate.meteoswiss.ch/idaweb), the topographical data by SwissTopo (no free distribution). We also would like to thank M. Zappa (WSL) for the monthly discharge data set [49], which corresponds to an improved version of the dataset that is currently published by the Swiss Federal Office for the environment [57] here: www.bafu.admin.ch/mq-gwn-ch-e (accessed on 9 July 2018).

Appendix A. Supplementary data

Supplementary data related to this article can be found at https://doi.org/10.1016/j.renene.2018.07.104.

References

[1] D. Gernaat, P.W. Bogaart, D.P. van Vuuren, H. Biemans, R. Niessink, High-resolution assessment of global technical and economic hydropower potential, Nature Energy 2 (2017).
[2] Eurostat, Renewable Energy Statistics, Figure 5: Gross Electricity Generation from Renewable Sources, EU-28, 2018, 1990–2016, available at: http://ec.europa.eu/eurostat/statistics-explained/index.php/Renewable_energy_statistics#30.25_of_electricity_generated_come_from_renewable_sources. (Accessed 11 July 2018).
[3] B. Lehner, G. Czisch, S. Vassolo, The impact of global change on the hydropower potential of Europe: a model-based analysis, Energy Pol. 33 (2005) 839–855.
[4] T.P. Barnett, J.C. Adam, D.P. Lettenmaier, Potential impacts of a warming climate on water availability in snow-dominated regions, Nature 438 (2005) 303–309.
[5] K. Bauermann, S. Spiecker, C. Weber, Individual decisions and system development – integrating modelling approaches for the heating market, Appl. Energy 116 (2014) 149–158.
[6] N. Voisin, M. Kintner-Meyer, R. Skaggs, T. Nguyen, D. Wu, J. Dirks, et al., Vulnerability of the US western electric grid to hydro-climatological conditions: how bad can it get? Energy 115 (2016) 1–12.
[7] B. Hamududu, A. Killingtveit, Assessing climate change impacts on global hydropower, Energies 5 (2012) 305–322.
[8] S.C. Kao, M.J. Sale, M. Ashfaq, R.U. Martinez, D.P. Kaiser, Y.X. Wei, et al., Projecting changes in annual hydropower generation using regional runoff data: an assessment of the United States federal hydropower plants, Energy 80 (2015) 239–250.
[9] B. Schaefli, Projecting hydropower production under future climates: a guide for decision-makers and modelers to interpret and design climate change impact assessments, WIREs Water 2 (2015) 271–289.
[10] N.S. Christensen, D.P. Lettenmaier, A multimodel ensemble approach to assessment of climate change impacts on the hydrology and water resources of the Colorado River Basin, Hydrol. Earth Syst. Sci. 11 (2007) 1417–1434.
[11] K. Madani, J.R. Lund, Estimated impacts of climate warming on California's high-elevation hydropower, Climatic Change 102 (2010) 521–538.
[12] T. Bolch, A. Kulkarni, A. Kääb, C. Huggel, F. Paul, J.G. Cogley, et al., The state and fate of himalayan glaciers, Science 336 (2012) 310–314.
[13] R.S. Bradley, M. Vuille, H.F. Diaz, W. Vergara, Threats to water supplies in the tropical andes, Science 312 (2006) 1755–1756.
[14] B. Orlove, glacier retreat reviewing the limits of human adaptation to climate change, Environment 51 (2009) 22–34.
[15] L. Gaudard, F. Romerio, F. Dalla Valle, R. Gorret, S. Maran, G. Ravazzani, et al., Climate change impacts on hydropower in the Swiss and Italian Alps, Sci. Total Environ. 493 (2014) 1211–1221.
[16] B. Schaefli, B. Hingray, A. Musy, Climate change and hydropower production in the Swiss Alps: quantification of potential impacts and related modelling uncertainties, Hydrol. Earth Syst. Sci. 11 (2007) 1191–1205.
[17] W. Vergara, A. Deeb, A. Valencia, R Bradley, B. Francou, A. Zarzar, et al., Economic impacts of rapid glacier retreat in the Andes. EOS, Trans. Am. Geophys. Union 88 (2007) 261–264.
[18] M. Beck, M. Scherer, SwissGrid - overview of ancillary services, available at: https://www.swissgrid.ch/dam/swissgrid/customers/topics/ancillary-services/as-documents/D100412-AS-concept-V1R0-en.pdf, 2010. (Accessed 9 July 2018). Frick, Switzerland p. 6.
[19] Swiss Federal Office for Energy, Swiss Electricity Statistics 2016. Annual Report, 2017, p. 56, available at: http://www.bfe.admin.ch/themen/00526/00541/00542/00630/index.html?lang=en. (Accessed 9 July 2018). time series available upon direct request. Bern: Swiss Federal Office for Energy.
[20] M. Fischer, M. Huss, M. Hoelzle, Surface elevation and mass changes of all Swiss glaciers 1980-2010, Cryosphere 9 (2015) 525–540.
[21] M. Pfaundler, M. Zappa, Die mittleren Abflüsse über die ganze Schweiz - Ein optimierter Datensatz im 500×500 m Raster, available at: https://www.bafu.admin.ch/bafu/de/home/themen/wasser/zustand/karten/mittlerer-monatlicher-und-jaehrlicher-abfluss/mittlere-monatliche-und-jaehrliche-abflusshoehen.html, 2008. (Accessed 9 July 2018).
[22] M. Huss, R. Hock, A new model for global glacier change and sea-level rise, Front. Earth Sci. 3 (2015).
[23] M. Balmer, Nachhaltigkeitsbezogene Typologisierung der schweizerischen Wasserkraftanlagen - GIS-basierte Clusteranalyse und Anwendung in einem Erfahrungskurvenmodell, Zürich: ETHZ, 2012.
[24] P. Blanc, B. Schädler, Water in Switzerland - an overview, available in English on http://www.naturalsciences.ch/topics/water/, , 2013. (Accessed 9 July 2018). Bern p. 28.
[25] R. Weingartner, H. Aschwanden, Discharge regime - the basis for the estimation of average flows. Plate 5.2, in: R. Weingartner, M. Spreafico (Eds.), Hydrological Atlas of Switzerland, 1992. http://hades.unibe.ch. (Accessed 9 July 2018). Bern.
[26] P. Hänggi, R. Weingartner, Variations in discharge volumes for hydropower generation in Switzerland, Water Resour. Manag. 26 (2012) 1231–1252.
[27] M. Huss, D. Farinotti, A. Bauder, M. Funk, Modelling runoff from highly glacierized alpine drainage basins in a changing climate, Hydrol. Process. 22 (2008) 3888–3902.
[28] D. Farinotti, S. Usselmann, M. Huss, A. Bauder, F. M, Runoff evolution in the Swiss Alps: projections for selected high-alpine catchments based on ENSEMBLES scenarios, Hydrol. Process. 26 (2012) 1909–1924.
[29] P. Horton, B. Schaefli, B. Hingray, A. Mezghani, A. Musy, Assessment of climate change impacts on Alpine discharge regimes with climate model uncertainty, Hydrol. Process. 20 (2006) 2091–2109.
[30] D. Finger, G. Heinrich, A. Gobiet, A. Bauder, Projections of future water resources and their uncertainty in a glacierized catchment in the Swiss Alps and the subsequent effects on hydropower production during the 21st century, Water Resour. Res. 48 (2012). W02521.
[31] N. Addor, O. Rössler, N. Köplin, M. Huss, R. Weingartner, J. Seibert, Robust changes and sources of uncertainty in the projected hydrological regimes of Swiss catchments, Water Resour. Res. 50 (2014) 7541–7562.
[32] Swiss Federal Office for Energy. Statistics of the Swiss hydropower facilities - Statistik der Wasserkraftanlagen der Schweiz (WASTA), state 01. 01. 2017, available on http://www.bfe.admin.ch/geoinformation/05061/05249/index.html?lang=de&dossier_id=01049 (last accessed 09 July 2018). Bern, Switzerland: Swiss federal Office for energy; 2017.
[33] Swiss Federal Office for Energy, Dams and reservoirs under the supervision of the federal government, Home > Geodata > Dams and reservoirs or, http://www.bfe.admin.ch, 2018. (Accessed 9 July 2018), http://www.bfe.admin.ch/geoinformation/05061/05251/index.html?lang=en. Bern, Switzerland: Swiss Federal Office for Energy.
[34] P. Manso, B. Schaefli, A.J. Schleiss, Adaptation of Swiss hydropower infrastructure to meet future electricity needs, in: Proceedings of Hydro 2015-Advancing policy and practice, Bordeaux, 26–28 Oct. 2015, Hydropower & Dams, Aqua Media International Ltd, Wallington, 2015.

[35] A.B. Gurung, A. Borsdorf, L. Fureder, F. Kienast, P. Matt, C. Scheidegger, et al., Rethinking pumped storage hydropower in the european Alps a call for new integrated assessment tools to support the energy transition, Mt. Res. Dev. 36 (2016) 222–232.
[36] S. Fatichi, S. Rimkus, P. Burlando, R. Bordoy, P. Molnar, High-resolution distributed analysis of climate and anthropogenic changes on the hydrology of an Alpine catchment, J. Hydrol. 525 (2015) 362–382.
[37] S. Terrier, M. Bieri, F. Jordan, A.J. Schleiss, Impact of glacier shrinkage and adapted hydropower potential in the Swiss Alps, Houille Blanche-Rev Int (2015) 93–101.
[38] T. Wagner, M. Themeßl, A. Schüppel, A. Gobiet, H. Stigler, S. Birk, Impacts of climate change on stream flow and hydro power generation in the Alpine region, Environmental Earth Sciences 76 (2016) 4.
[39] M. Huss, G. Jouvet, D. Farinotti, A. Bauder, Future high-mountain hydrology: a new parameterization of glacier retreat, Hydrol. Earth Syst. Sci. 14 (2010) 815–829.
[40] J. Gabbi, D. Farinotti, A. Bauder, H. Maurer, Ice volume distribution and implications on runoff projections in a glacierized catchment, Hydrol. Earth Syst. Sci. 16 (2012) 4543–4556.
[41] FOEN, Effects of Climate Change on Water Resources and Waters. Synthesis Report on “Climate Change and Hydrology in Switzerland” (CCHydro) Project, 2012, p. 74. Results also available at: https://hydro.slf.ch/sihl/cchydro/#. (Accessed 26 February 2016). Bern: Federal Office for the Environment.
[42] CHy SGHL, Auswirkungen der Klimaänderung auf die Wasserkraftnutzung – Synthesebericht. Beiträge zur Hydrologie der Schweiz, Nr 38. Bern: Swiss Society of Hydrology and Limnology (SGHL) and Swiss Hydrological Commission (CHy), 2011, p. 28.
[43] D. Farinotti, A. Pistocchi, M. Huss, From dwindling ice to headwater lakes: could dams replace glaciers in the European Alps? Environ. Res. Lett. (2016) 11, 054022.
[44] M.J.R. Speich, L. Bernhard, A.J. Teuling, M. Zappa, Application of bivariate mapping for hydrological classification and analysis of temporal change and scale effects in Switzerland, J. Hydrol. 523 (2015) 804–821.
[45] M. Huss, M. Zemp, P.C. Joerg, N. Salzmann, High uncertainty in 21st century runoff projections from glacierized basins, J. Hydrol. 510 (2014) 35–48.
[46] L. Langhammer, L. Rabenstein, A. Bauder, H. Maurer, Ground-penetrating radar antenna orientation effects on temperate mountain glaciers, Geophysics 82 (2017) H15–H24.
[47] A. Schleiss, ROADMAP Hydropower, Swiss Competence Center on Energy Research - Supply of Energy, 2014. http://www.sccer-soe.ch/en/aboutus/roadmaps/. (Accessed 9 July 2018).
[48] Swiss Federal Office for Energy, Swiss electricity statistics 2015, available at: http://www.bfe.admin.ch/themen/00526/00541/00542/00630/index.html?lang=en, 2016. (Accessed 14 July 2016). Bern: Swiss Federal Office for Energy p. 56.
[49] M. Zappa, L. Bernhard, F. Fundel, S. Joerg-Hess, Vorhersage und Szenarien von Schnee- und Wasserressourcen im Alpenraum, 2012, pp. 19–27. Data set available from: the lead author. Forum für Wissen.
[50] Swiss Federal Office for the Environment, Mean monthly and annual runoff depths, digital data set, available at: https://www.bafu.admin.ch/bafu/en/home/topics/water/state/maps/mean-monthly-and-annual-runoff/mean-monthly-and-annual-runoff-depths.html. (Accessed 9 July 2018). Bern 2013.
[51] M. Fischer, M. Huss, C. Barboux, M. Hoelzle, The New swiss glacier inventory SGI2010: relevance of using high-resolution source data in areas dominated by very small glaciers, Arctic Antarct. Alpine Res. 46 (2014) 933–945.
[52] D.P. Dee, S.M. Uppala, A.J. Simmons, P. Berrisford, P. Poli, S. Kobayashi, et al., The ERA-Interim reanalysis: configuration and performance of the data assimilation system, Q. J. R. Meteorol. Soc. 137 (2011) 553–597.
[53] K.E. Taylor, R.J. Stouffer, G.A. Meehl, An overview of CMIP5 and the experiment, Bull. Am. Meteorol. Soc. 93 (2012) 485–498.
[54] L. Tonka, Hydropower license renewal and environmental protection policies: a comparison between Switzerland and the USA, Reg. Environ. Change 15 (2015) 539–548.
[55] Grande Dixence, Grande Dixence - experience the energy at the heart of the Alps. http://www.grande-dixence.ch/docs/default-source/documentation/grande-dixence/Grande-Dixence-Experience-the-energy-at-the-heart-of-the-Alps.pdf?sfvrsn=9, 2010. (Accessed 9 July 2018). Sion: Grande Dixence SA P. 49.
[56] M. Kummer, M. Baumgartner, D. Devanthéry, Restwasserkarte. Schweiz. Wasserentnahmen und -rückgaben, 2007, p. 90, available, https://www.bafu.admin.ch/bafu/de/home/themen/wasser/publikationen-studien/publikationen-wasser/restwasserkarte-schweiz.html. (Accessed 9 July 2018). Bern, Switzerland: Swiss Federal Office for the Environment.
[57] Swiss Federal Office for the Environment (FOEN), Dataset MQ-GWN-CH, modeled natural runoff means for the Swiss river network, available at: https://www.bafu.admin.ch/bafu/en/home/topics/water/state/maps/mean-monthly-and-annual-runoff/mean-runoff-and-flow-regime-types-for-the-river-network-of-switz.html, 2013. (Accessed 9 July 2018). Bern: Swiss Federal Office for the Environment, FOEN.
[58] Swiss Federal Office for Energy, Statistics of the Swiss hydropower facilities - Statistik der Wasserkraftanlagen der Schweiz (WASTA), state 01. 01. 2015, 2015 available at: http://www.bfe.admin.ch/geoinformation/05061/05249/index.html?lang=de&dossier_id=01049. (Accessed 9 July 2018). Bern, Switzerland: Swiss Federal Office for Energy.
[59] SwissTopo, DHM25- the Digital Height Model of Switzerland, 2005. Wabern, Switzerland.
[60] SwissTopo, Vector25-The Digital Landscape Model of Switzerland, 2008. Wabern, Switzerland.
[61] B. Schädler, R. Weingartner, Components of the Natural Water Balance. Hydrologic Atlas of Switzerland - Plate 6.3, 2002. Available at: http://www.hades.unibe.ch/. (Accessed 9 July 2018). Bern: Service Hydrologique et Géologique National (SHGN).
[62] MeteoSwiss, Automatic Monitoring Network SWISSMETNET, 2018 available at: https://www.meteoswiss.admin.ch/home/measurement-and-forecasting-systems/land-based-stations/automatisches-messnetz.html. (Accessed 9 July 2018). Zurich.